Article:
Toric, N, Glavinić, I.U. and Burgess, I orcid.org/0000-0001-9348-2915 (2018) Development Of A Rheological Model For Creep Strain Evolution In Steel And Aluminium At High Temperature. Fire and Materials, 42 (8). pp. 879-888. ISSN 0308-0501

https://doi.org/10.1002/fam.2643

DEVELOPMENT OF A RHEOLOGICAL MODEL FOR CREEP STRAIN EVOLUTION IN STEEL AND ALUMINIUM AT HIGH TEMPERATURE

Neno Torić[1*], Ivana Uzelac Glavinić[1] and Ian W. Burgess[2]

Abstract:

The paper presents a rheological model capable of reproducing the temperature-, stress- and time-dependent strain component which occurs in steel and aluminium during exposure to high temperature. The model is capable of providing the creep strain output for the primary, secondary and tertiary creep phases for both steel and aluminium. Constitutive parameters of the rheological model are calibrated using two recent coupon test studies based on the European steel grade S275JR and aluminium grade EN6082AW T6, both of which are currently used in the construction industry. The calibrated constitutive parameters are valid within the temperature range within which creep is expected to occur (400-600°C for steel and 200-300°C for aluminium). The rheological model proposed in the paper can easily be used for application in finite-element-based computer codes.

Keywords:

Rheological model, Creep properties, Steel, Aluminium, High temperature, Fire

---

[1] University of Split, Faculty of Civil Engineering, Architecture and Geodesy, Matice Hrvatske 15, 21000 Split, Croatia, Tel: +385-21-303-366, Fax: +385-21-303-331

** E-mail: neno.toric@gradst.hr (corresponding author)*

[2] University of Sheffield, Department of Civil and Structural Engineering, Sir Frederick Mappin Building, Mappin Street, Sheffield, S1 3JD, UK.

1. INTRODUCTION

The influence of creep on the behaviour of metallic structures exposed to fire currently represents an open area for scientific research. Development of creep strain in steel and aluminium when exposed to fire temperatures can be expected to occur if the exposure to high temperature is prolonged. This is bound to occur when steel or aluminium is subjected to heating rates lower than 20°C/min, which certainly covers cases when the material is fire-protected or exposed to a slow-burning fire. In these cases the evolution of creep strain depends on the concurrent levels of stress and temperature and will ultimately have an adverse effect on the structural load-bearing system. This effect is manifested through overall reduction of the fire resistance of the structure or its constituent members. Generally, strain components in metallic materials during fire exposure are comprised of three parts [1]:

$$\varepsilon_{tot} = \varepsilon_{th}(T) + \varepsilon_{\sigma}(\sigma, T) + \varepsilon_{cr}(\sigma, T, t) \tag{1}$$

where: ε_{tot} – total strain, $\varepsilon_{th}(T)$ – temperature-dependent thermal strain, $\varepsilon_{\sigma}(\sigma,T)$ – stress related strain (also a function of temperature) and $\varepsilon_{cr}(\sigma,T,t)$ –creep strain. The creep strain is dependent on all three variables (time, temperature and stress), which makes it the most complex of the strain components. Furthermore, as the strain component which is time-dependent, the creep strain is the only component which depends heavily on the shape of the fire temperature-time curve which heats the material.

Creep in metallic materials starts to evolve during their exposure to stress. Creep is especially pronounced when the material is exposed to high temperature, although at ambient temperature it is usually, and justifiably, considered negligible. During high temperature exposure the deformation mechanism is more pronounced, since the atomic movement in the crystal lattice becomes substantial. The most important microscopic deformation mechanisms enabling creep strain are: dislocation glide in the crystal lattice, dislocation climb, sliding of the boundaries of crystal grains, and the diffusion of atoms and voids in the lattice [2]. Dislocation climb, during which the 'climb' of a dislocation to an adjacent free

slip plane occurs, presents the most important deformation mechanism for the manifestation of creep at high temperature.

Generally, there are three main creep phases during exposure to a constant stress and temperature. In the primary creep stage the creep strain rate is relatively high, but decreases with time. During the secondary phase the creep strain rate gradually becomes constant; this is also known as steady-state creep. During the tertiary phase the creep strain rate increases exponentially with time until steel rupture occurs. At higher temperatures and stress levels, the boundaries between the three stages are not as evident as they are at lower temperatures and stresses.

At present, the most commonly used rheological models used for representing creep are the Burgers [3] and ‘’standard’’ [4] solid models, which are generally used to model the primary and secondary creep phases only. These models are limited by their feasible shapes for the creep curve and by their inability to model the tertiary creep phase. The main motivation for this research is to expand the capabilities of rheological modelling by defining a model which can incorporate the tertiary phase. This paper proposes a modification of a non-linear rheological model consisting of a spring and a Kelvin-Voight element which can be applied to modelling all three creep phases of the high-temperature behaviour of steel and aluminium. Furthermore, the proposed model is suitable for implementation within finite element code for numerical modelling of structural behavior in fire.

2. PREVIOUS RESEARCH

Previously conducted research on the effects of creep at high temperature has mostly focused on conducting experimental creep-test studies on coupons of various steel and aluminium grades. The influence of creep on flush end-plate steel connections in fire has recently been studied by El Ghor *et al.* [5]. Recent creep-related research within the past two years has been conducted by Gales *et al.* [6] on the BS5896-compliant steels used in prestressing tendons. Further studies have been conducted by Wang *et al.* [7] on the Chinese grade Q345, and by Kodur and Aziz [8] on the American steel grade A572. This research has relied mostly on stationary creep tests (with the exception of study [5] in which transient creep tests were conducted). The creep behaviour of British and European steel grades was previously investigated by Kirby and Preston [9], Rubert and Schaumann [10] (transient tests on grades S235 and S355), Brnić *et al.* [11] and Torić *et al.* [12] (stationary tests on grade S275). Creep research on the aluminium alloy series 6xxx, which is used in the construction industry, was extensively investigated by Maljaars *et al.* [13] (Alloy 6060-T66), Langhele [14], Eberg *et al.* [15] (Alloys 6082 T4 and 6082 T6) and Torić *et al.* [16] (Alloy EN6082AW T6). Some research has also been carried out on the influence of creep on larger-scale specimens.

The reduction of fire resistance due to the presence of creep in steel beams and columns has been documented in research conducted by Torić *et al.* [17-18], Kodur *et al.* [19], and by Li and Zhang [20]. A general behaviour pattern observed in these studies was that creep increases deflections, which ultimately results in a reduction of fire resistance. This is evident both in cases when steel beams are restrained and when they are unrestrained.

The most frequently-used semi-empirical creep model for calibration of both stationary and transient creep tests was developed in 1967 by Harmathy [21]; this can be expressed in the form:

$$\varepsilon_{cr} = \frac{\varepsilon_{cr,0}}{0.693} \cdot cosh^{-1}\left(2^{\frac{Z\theta}{\varepsilon_{cr,0}}}\right) \qquad \left(\theta < \theta_0\right) \tag{2}$$

$$\varepsilon_{cr} = \varepsilon_{cr,0} + Z\theta \qquad \left(\theta \geq \theta_0\right) \tag{3}$$

$$\theta_0 = \varepsilon_{cr,0} / Z \tag{4}$$

in which $\varepsilon_{cr,0}$ is the length of the intersection between the creep curve in the secondary phase and the ordinate axis (derived from stress-controlled tests), and Z is the Zener-Hollomon parameter (h^{-1}). Variable θ represents temperature-compensated time [22] which takes into account the time-variation of temperature and is expressed as:

$$\theta = \int_0^t exp^{\frac{-\Delta H}{RT_R}} dt \tag{5}$$

in which ΔH is the creep activation energy (J/mol), T is the temperature (K) and R is the universal gas constant (J/molK). A model described by Equation (2) is based on a time-hardening rule which assumes that creep explicitly depends on time and stress level.

In order to present the capabilities of the proposed rheological model, two recent creep test studies have been chosen for calibration, since they offer complete stationary creep test results which are presented in a form of a simple analytical formula. These studies refer to creep tests conducted by Torić *et al.* [12] on steel grade S275JR and aluminium grade EN6082AW T6 [16]. Both studies used the same test methodology for determining stationary creep.

The purpose of both of the studies [12] and [16] was to determine material parameters and time-dependent creep strain values in the temperature ranges 400-600°C and 200-300°C for steel S275 and aluminium EN6082AW T6 respectively. The test regime consisted of three phases in each case:

1. Heating phase with an approximate heating rate of 15°C/min,
2. Soaking period which lasted 60 minutes,
3. Loading phase in which the stress and temperature levels were held constant.

In these studies constant-stress-rate tests at 10 MPa/s were also conducted in order to obtain the modulus of elasticity, stress at 0.2% strain and stress-strain curves within the temperature ranges 20-600°C for steel and 20-350°C for aluminium. The soaking period for the constant-stress-rate tests was 30 minutes. The results from the creep and constant-stress-rate tests were used in order to calibrate the constitutive components of the rheological model, which are presented in Section 4 of the paper.

3. THE RHEOLOGICAL MODEL

3.1 Constitutive equations

The basic concept of the rheological model was adapted from the study of Helman and Creus [23], whose original intention was to define a rheological model for non-linear time-dependent strain under constant stress at ambient temperature. The authors of this paper have modified the original rheological model and adapted it so that it can represent the creep behaviour of steel and aluminium when exposed to high temperature.

The rheological model consists of two elements in series, as shown in Fig. 1(a). The first rheological element (Spring Element 1) represents a stress-related strain component. The constitutive model for this spring element is represented by the general nonlinear stress (σ_1) – strain (ε_1) relationship:

$$\sigma_1 = \mathrm{E}_1(\mathrm{T})\varepsilon_1(\ 1-\beta_1(\sigma,\mathrm{T})\varepsilon_1) \quad ; \quad 0 \le \varepsilon_1 \le 1/\beta_1 \tag{6}$$

in which E_1 represents the temperature-dependent modulus of elasticity of Spring 1. Maximum stress and stress-related strain can be expressed as:

$$\sigma_{1\max} = \mathrm{E}_1(\mathrm{T})/4\beta_1(\sigma,\mathrm{T}) \quad ; \quad \varepsilon_{\mathrm{u}1} = 1/\beta_1 \tag{7}$$

The second rheological element is of the Kelvin-Voight type, and represents the creep stress and strain. In this component's Equation (8) the total stress of the element (σ_2) represents the sum of the stresses in the Spring Element 2 and the dashpot K:

$$\sigma_2 = \mathrm{E}_2(\mathrm{T})\varepsilon_2(\ 1-\beta_2(\sigma,\mathrm{T})\varepsilon_2) + \mathrm{K}(\sigma,\mathrm{T})\dot{\varepsilon}_2 \quad ; \quad 0 \le \varepsilon_2 \le 1/\beta_2 \tag{8}$$

in which E_2 is the temperature-dependent modulus of elasticity of Spring 2, ε_2 is the strain of the second rheological element, K is the temperature- and stress-dependent constant of the dashpot. β_2 can be expressed with the help of a maximum strain (ε_{u2}) as $\varepsilon_{u2}=1/\beta_2$. The

definitions of the stress-strain relationships for the springs of both rheological elements is presented in Fig 1(b).

If exposed to constant stress and temperature, the total strain can be expressed as the sum of the stress-related and creep strains:

$$\varepsilon_{\text{tot}} = \varepsilon_1 + \varepsilon_2 = \varepsilon_\sigma\left(\sigma, \mathrm{T}\right) + \varepsilon_{\text{cr}}\left(\sigma, \mathrm{T}, \mathrm{t}\right) \tag{9}$$

The thermal strain component is not included in this analysis, since it is only temperature-dependent and can be treated as independent of the stress and time variables.

3.2 Stress-related strain

When considering the case of constant stress $\sigma(t)=\sigma_0$ applied at time $t=0$, the stress-related strain, represented by the first element, which is derived from Equation (6) can be expressed as:

$$\varepsilon_1 = \varepsilon_\sigma = \frac{1}{2\beta_1}\left[1 - \sqrt{\left(1 - \frac{\sigma_0}{\sigma_1^{\max}}\right)}\right];\ 0 \le \varepsilon_1 \le \frac{1}{2\beta_1} \tag{10}$$

As can be seen from Fig. 1b, the shape of the stress-strain curve is parabolic, which does not represent very well the behaviour of steel or aluminium. A general stress-strain model for steel in fire was proposed by Eurocode 3, Part 1.2 [24], which consists of three parts: linear, elliptic and a yield plateau. This type of stress-strain law contains an implicit creep component, and a modification of this model to remove the implicit creep component was proposed by Torić *et al.* [25]. A general stress-related strain model for aluminium in fire is based on a Ramberg-Osgood type of curve [26], since the shape of a typical stress-strain curve for aluminium is different from that of steel.

3.3 Creep strain under constant stress

At constant stress, the strain corresponding to the second element can be derived from Equation (8) as the solution of the second-order linear equation:

$$\dot{\varepsilon}_2 - \frac{\mathrm{E}_2(\mathrm{T})\beta_2(\sigma,\mathrm{T})}{\mathrm{K}(\sigma,\mathrm{T})}\varepsilon_2^2 + \frac{\mathrm{E}_2(\mathrm{T})}{\mathrm{K}(\sigma,\mathrm{T})^2}\varepsilon_2 = \frac{\sigma_0}{\mathrm{K}(\sigma,\mathrm{T})} \tag{11}$$

The solution of Equation (11) depends on the value of the parameter γ, defined as:

$$\gamma = \frac{4\beta_2(\sigma,\mathrm{T})\sigma_0}{\mathrm{E}_2(\mathrm{T})} = \frac{\sigma_0}{\sigma_{2\max}} \tag{12}$$

If $\gamma < 1$:

$$\varepsilon_2 = \varepsilon_{\mathrm{cr}} = \frac{1}{2\beta_2}\left[1 - \sqrt{(1-\gamma)}\,\frac{1+\sqrt{(1-\gamma)} + \left[1-\sqrt{(1-\gamma)}\right]\exp^{-\mathrm{E}_2/\mathrm{K}\sqrt{(1-\gamma)}\mathrm{t}}}{1+\sqrt{(1-\gamma)} - \left[1-\sqrt{(1-\gamma)}\right]\exp^{-\mathrm{E}_2/\mathrm{K}\sqrt{(1-\gamma)}\mathrm{t}}}\right] \tag{13}$$

If $\gamma = 1$:

$$\varepsilon_2 = \varepsilon_{\mathrm{cr}} = \frac{1}{2\beta_2}\left(\frac{\mathrm{t}}{\frac{2\mathrm{K}}{\mathrm{E}_2} + \mathrm{t}}\right) \tag{14}$$

If $\gamma > 1$:

$$\varepsilon_2 = \varepsilon_{\mathrm{cr}} = \frac{1}{2\beta_2}\left[\gamma\,\frac{1+\sqrt{(\gamma-1)}\sin\mathrm{E}_2/\mathrm{K}\sqrt{(\gamma-1)}\ \mathrm{t} - \cos\mathrm{E}_2/\mathrm{K}\sqrt{(\gamma-1)}\ \mathrm{t}}{\gamma + 2\sqrt{(\gamma-1)}\sin\mathrm{E}_2/\mathrm{K}\sqrt{(\gamma-1)}\ \mathrm{t} + (\gamma-2)\cos\mathrm{E}_2/\mathrm{K}\sqrt{(\gamma-1)}\ \mathrm{t}}\right] \tag{15}$$

In the proposed modification of the rheological model the value of the parameter γ determines whether the tertiary creep phase exists. If $\gamma \leq 1$ only the primary and the secondary creep phases will occur, while if $\gamma > 1$ the tertiary creep phase will manifest itself as part of the total strain output.

4. CALIBRATION OF THE CONSTITUTIVE COMPONENTS OF THE RHEOLOGICAL MODEL

4.1 General assumptions

In order to properly calibrate the proposed rheological model a few assumptions need to be made regarding the test results which are being used for calibration:

- An estimate of the minimum stress level at which tertiary creep starts to occur at each temperature level needs to be defined,

- In cases where all three creep phases occur the maximum strain ε_{max} is assumed to be constant at any prescribed temperature level.

4.2 Calibration of the rheological model for steel S275JR

By adopting the test values [12] for the modulus of elasticity (E_1) and the stress at 0.2% strain (σ_{1max}), shown in Table 1, the material model for Spring 1 can be defined. A comparison between the stress-related strain obtained from the Spring 1 model and the test values is presented in Fig. 2.

Creep test results [12] were used in order to calibrate the second element of the rheological model. Since creep tests are based on constant stress, the stress-related strain is also constant. As can be seen from Fig. 1 (a), failure occurs after the total strain exceeds the maximum test strain:

$$\varepsilon_{\max} = \varepsilon_1 + \varepsilon_{u2} \tag{16}$$

By adopting the experimental values for ε_{max} from stationary creep tests (i.e. the maximum recorded strain for any prescribed temperature level), the ultimate strain of Spring 2 (ε_{u2}) for each temperature level can easily be obtained. The experimental values of the maximum strain at each stress and temperature level from study [12] are presented in Table 2. The smallest value of the maximum strain for each temperature level was adopted as ε_{max}.

Since the parameter γ, as defined by Equation (12), governs the development of the tertiary creep phase, σ_{2max} is defined as the minimum stress level at which the tertiary creep phase starts to occur. By determining ε_{u2} and σ_{2max} from test results, the model for Spring 2 (Fig. 1(b)) can be defined. As observed from Table 2, at 400°C there is no tertiary creep phase within the experimental stress range, while at 500°C and 600°C the coupons experienced the tertiary creep phase at all stress levels. This indicates that the following can be assumed: at 400°C $\sigma_{2max} \geq 0.9\sigma_{1max}$, at 500°C $\sigma_{2max} \leq 0.45\sigma_{1max}$ and at 600°C $\sigma_{2max} \leq 0.25\sigma_{1max}$. Hence, using the available data, σ_{2max} was chosen as: a) at 400°C $\sigma_{2max}=0.9\sigma_{1max}$; b) at 500°C $\sigma_{2max}=0.45\sigma_{1max}$; c) at 600°C $\sigma_{2max}=0.25\sigma_{1max}$.

In order to calibrate the dashpot component, the model for parameter K was obtained by a curve-fitting process using the stationary creep test results [12] with the help of Equations (13)-(15). From Table 2 it can be seen that at 400°C there was no rupture of the steel coupon due to creep, even at high stress levels, so Equation (16) is not valid for defining ε_{u2} at 400°C. Fig. 3 (a-b) shows the influence of parameters ε_{u2} and K on the total strain calculated from Equations (10) and (13).

As shown in Fig. 3, for $\gamma < 1$ the parameter ε_{u2} influences the maximum strain value, which is constant because there is no tertiary creep phase, and the parameter K influences the steepness of the primary creep phase. Therefore, at 400°C ε_{u2} can be determined by fitting the experimental maximum strain, while parameter K can be determined so that the model closely represents the primary creep phase obtained by experiments. The results obtained by using the parameters that are determined in this fashion are presented in Fig. 4.

Figs. 5 and 6 present a comparison between the proposed rheological model and stationary creep tests at 500°C and 600°C. As mentioned earlier, the values of σ_{2max} are taken as $0.45\sigma_{1max}$ at 500°C and $0.25\sigma_{1max}$ at 600°C, while maximum strain values are 12.4% and 6.6% respectively, as shown in Table 2. Consequently, ε_{u2} is obtained from Equation (16), while K is determined by fitting the creep test results. Values of the parameter K used for obtaining the results shown in Figs 5 and 6 are presented in Table 3.

Fig. 7 is a plot of the stress-strain curves for the first and the second springs, for all temperature and stress levels. At 400 °C, where there is no tertiary creep phase, the model for Spring 2 is very much dependent on the stress level. At 500 °C and 600 °C the assumption that ε_{max} is the minimum total test strain value provides a good match with the creep tests. It can be observed that there is no significant difference between the stress-strain behaviour of Spring 2 with respect to stress at each temperature level.

4.3 Calibration of the rheological model for aluminium EN6082AW T6

The results of the constant stress-rate tests from study [16] were used in order to calibrate the model of Spring 1 and to adapt the rheological model to the mechanical properties of aluminium alloy EN6082AW T6. The test values for modulus of elasticity (E_1) and stress at 0.2% strain (σ_{1max}) are presented in Table 4. Using these values the constitutive

model for Spring 1 can be defined for all temperature levels. A comparison between the experimental [16] and predicted stress-strain curves of Spring 1 of the proposed rheological model is presented in Fig. 8.

The experimental values [16] of maximum test strain at each stress and temperature level are presented in Table 5. At a stress level of 38.1 MPa, where there is little creep present, the total strain is almost equal to the stress-related strain within a 240-minute interval. As is the case with steel, the smallest value of maximum test strain at each temperature level was adopted as ε_{max}, meaning that the ultimate strain of Spring 2 (ε_{u2}) for each temperature level can easily be obtained with the help of Equation (16). At 200°C ε_{max} was chosen as 1.8%, since that was the highest value of creep strain, obtained after 1200 minutes of the creep test at 200°C [16]. As can be seen from Table 5, at 200°C the tertiary creep phase occurs between $0.3\sigma_{1max}$ and $0.5\sigma_{1max}$, while at 300°C the tertiary creep phase occurs between $0.15\sigma_{1max}$ and $0.30\sigma_{1max}$. With respect to the available creep data, at 200°C σ_{2max} was chosen to be $0.5\sigma_{1max}$. Fig. 9 presents a comparison between the prediction of the rheological model and creep tests at 200°C. Parameter K is again determined by fitting the test results. Fig. 10 presents a comparison between the predictions of the rheological model and creep tests at 250°C. As the creep tests suggest, σ_{2max} was chosen to be $0.3\sigma_{1max}$ while ε_{u2} was chosen to be 0.78% (Table 5).

Figs. 11 and 12 present a comparison between the proposed rheological model at 300°C and the corresponding creep tests for stress levels of $0.30\sigma_{1max}$ and $0.50\sigma_{1max}$. Since we know from the tests that the tertiary creep phase occurs somewhere between $0.15\sigma_{1max}$ and $0.30\sigma_{1max}$, we can assume that $\sigma_{2max}=0.30\sigma_{1max}$. However, for this assumption the rheological model shows significant discrepancies with the creep tests. In order to clarify the cause of these discrepancies, Figs. 11 and 12 present the model's results for different values of the parameters K and σ_{2max}. It can be seen from these figures that changes in σ_{2max} have a significant influence on the time at which the tertiary phase begins, while changes in K very much reflect the gradient at the start of the creep curve. Therefore, by selecting K as an approximation to the initial tangent, it can be seen that σ_{2max} needs to have a value less than $0.30\sigma_{1max}$ in order to reduce the discrepancies. Values of the parameter K for aluminium at different temperature levels are presented in Table 6.

Fig. 13 presents the stress-strain models for Springs 1 and 2 in the case of aluminium. In similar fashion to steel, at stress levels where only the primary creep phase is present, ε_{u2} is obtained by curve-fitting the total strain with the creep tests.

5. COMPARISON WITH OTHER TEST STUDIES

5.1 Comparison with other creep studies of grade S275 steel

Fig. 14 presents a comparison between the predictions of the proposed rheological model and creep tests conducted by Brnić et al. [11] on grade S275 steel. In this exercise only the first spring was calibrated using the test results (stress at 0.2% strain and modulus of elasticity at the prescribed temperature level) from [12]. It can be seen from the figure that there is some discrepancy between the predictions of rheological model and the creep tests from [11]. This can be explained by the fact that the Kelvin-Voight element was not calibrated using the test results from [11]. The values of maximum test strain recorded in the creep tests in [11] are different from those recorded in [12]. Since the second rheological element governs the creep behaviour, this represents the main reason for the discrepancy.

5.2 Comparison with other creep studies of aluminium alloy EN6082AW T6

Fig. 15 presents a comparison between the predictions of the proposed rheological model and creep tests conducted by Langhele [14] on aluminium alloy 6082 T6. Only the data for modulus of elasticity and stress at 0.2% strain were used for calibration of Spring 1. It can be seen that the correlation between the model and tests is much better in this case, which indicates that the calibration of the second Kelvin-Voight element with regard to creep development is satisfactory.

5.3 Applicability of the proposed rheological model

Considering the comparisons given in 5.1 and 5.2, it can be seen that the rheological model, with the current calibration of its constitutive components, produces strain outputs which are comparable to the test results from similar coupon studies. The total time interval

chosen for comparison is four hours, since this represents a typical reference time-frame for general fire exposure cases.

The precision of the rheological model very much depends on the extent to which the input parameters from other studies vary in comparison to parameters obtained from the coupon studies [12] and [16] which have been used here. More precise calibration factors for a prescribed alloy can be obtained if the total interval for constant-temperature creep tests is shortened, or the stress levels at which the creep tests are conducted are increased at all temperature levels. It can be also seen that the assumptions imposed on test data in Section 4.1 are well formulated for adequate calibration of the Kelvin-Voight element.

Generally, the calibration procedure described in Section 4 can be applied to any metallic material which exhibits high-temperature creep, which makes the principles of the rheological model universal for modelling stationary creep tests at high temperatures. The formulas presented in Section 3 can easily be utilized for implementation in finite-element-based computer codes, allowing creep to be modelled explicitly in thermo-structural analyses.

6. CONCLUSION

The paper proposes a new type of rheological model, calibrated against steel S275JR and aluminium EN6082AW T6 at high temperatures, which takes into account all three distinct creep phases. The main motivations for development of this rheological model are to enable inclusion of the tertiary creep phase in high-temperature analysis of metallic materials and to provide a practical way for its implementation in finite-element-based codes. The following conclusions regarding the presented research can be postulated:

- The calibration procedure proposed in the paper is sufficiently accurate for adequate representation of creep strains of the selected steel and aluminium alloys at high temperatures;
- The rheological model provides very good correlation with a similar creep test study in the case of aluminium;
- The precision of the rheological model depends on the temperature- and stress-intervals used in the study selected for calibration;

- The rheological model can be considered as a universal model for reproducing stationary high-temperature creep tests of metallic materials within the first four hours of fire exposure.

Acknowledgement

This work has been fully supported by Croatian Science Foundation under the project *Influence of creep strain on the load capacity of steel and aluminium columns exposed to fire* (UIP-2014-09-5711). Any opinions, findings, and conclusions or recommendations expressed in this material are those of the authors and do not necessarily reflect the views of Croatian Science Foundation.

REFERENCES

[1] Anderberg, Y., "Modelling Steel Behaviour", *Fire Safety Journal,* 1988; 13(1):17-26.

[2] Lee J. and Gillie M., Numerical modelling of creep in structural steel exposed to fire, *7th International Conference on Structures in Fire*, Zurich, Switzerland, 449-458, 2012.

[3] Cowan M. and Khandelwal K., "Modelling of high temperature creep in ASTM A992 structural steels", *Engineering Structures*, 2014; 80:426-434.

[4] Brnić J., Turkalj G., Lanc D., Čanadija M., Brčić M., Vukelić G., "Comparison of material properties: Steel 20MnCr5 and similar steels, *Journal of Constructional Steel Research*, 2014, 95; 81–89.

[5] H. El Ghor A. and G. Hantouche E., "Thermal Creep Mechanical-based Modeling for Flush Endplate Connections in Fire", *Journal of Constructional Steel Research*, 2017; 136:11-23.

[6] Gales J., Robertson L. and Bisby L., "Creep of Prestressing Steels in Fire", *Fire and Materials,* 2016; 40(7):875-895.

[7] Wang W., Yan S. and Kodur V., "Temperature Induced Creep in Low-Alloy Structural Q345 Steel", *Journal of Materials in Civil Engineering,* 2016; 28(6), DOI: 10.1061/(ASCE)MT.1943-5533.0001519

[8] Kodur V. K. and Aziz E. M., "Effect of temperature on creep in ASTM A572 high-strength low-alloy steels", *Materials and Structures*, 2015, DOI: 10.1617/s11527-014-0262-2

[9] Kirby, B.R. and Preston, R.R., "High Temperature Properties of Hot-Rolled, Structural Steels for Use in Fire Engineering Design Studies", *Fire Safety Journal*, 1988, 13:27-37.

[10] Rubert, A. and Schaumann P., "Temperaturabhaengige Werkstoffeigenschaften von Baustahl bei Brandbeanspruchung", *Stahlbau*, 1985, 3, 81-86.

[11] Brnić J., Turkalj G., Jitai N., Čanađija M., Lanc D., "Analysis of experimental data on the behavior of steel S275JR – Reliability of modern design", *Materials and Design,* 2013; 47:497-504.

[12] Torić N., Brnić J., Boko I., Brčić M., Burgess I. W. and Uzelac Glavinić I., "Development of a High Temperature Material Model for Grade S275JR Steel", *Journal of Constructional Steel Research*, 2017; 137:161-168.

[13] Maljaars, J., Soetens, F. and Katgerman, L., "Constitutive model for aluminium alloys exposed to fire conditions", *Metallurgical and Materials Transactions A*, 2008, 39(4):778-789.

[14] Langhelle, N.K., Experimental validation and calibration of nonlinear finite element models for use in design of aluminium structures exposed to fire, PhD thesis, Norwegian University of Science and Technology, Trondheim, ISBN 82-471-0376-1, 1999.

[15] Eberg, E., Amdahl, J. and Langhelle, N.K., Experimental investigation of creep behaviour of aluminium at elevated temperatures, SINTEF report no. STF22 F96713, 1996.

[16] Torić N., Brnić J., Boko I., Brčić M., Burgess I. W. and Uzelac I., ''Experimental Analysis of the Behaviour of Aluminium Alloy EN6082 AW T6 at High Temperature'', *Metals*, 2017, 7, 126.

[17] Torić, N., Harapin, A. and Boko, I., "Experimental Verification of a Newly Developed Implicit Creep Model for Steel Structures Exposed to Fire", *Engineering Structures*, 2013; 57:116-124.

[18] Torić, N., Harapin A. and Boko I., "Modelling of the influence of creep strains on the fire response of stationary heated steel members", *Journal of Structural Fire Engineering*, 2015; 6(3), 155-176.

[19] Kodur V. K. R. and Dwaikat M. M. S., "Effect of High Temperature Creep on the Fire Response of Restrained Steel Beams", *Materials and Structures*, 2010; 43(10), 1327-1341.

[20] Li G.-Q. and Zhang C., "Creep effect on buckling of axially restrained steel columns in real fires", *Journal of Constructional Steel Research*, 2012; 71:182-188.

[21] Harmathy, T. Z., "A Comprehensive Creep Model", *Journal of Basic Engineering*, 1967, 89(3): 496-502.

[22] Dorn J. E., ''Some Fundamental Experiments on High Temperature Creep'', *Journal of the Mechanics and Physics of Solids*, 1955; 3(2):85-88

[23] Helman H. and Creus G. J., ''A non-linear rheological model describing time-dependant deformations and failure'', *International Journal of Non-Linear Mechanics*, 1975; 10:167-172.

[24] EN 1993-1-2:2005, *"Eurocode 3 – Design of steel structures – Part 1-2: General Rules – Structural fire design"*, European Committee for Standardization, Brussels, 2005.

[25] Torić, N., Sun R.R. and Burgess, I.W., "Creep-free fire analysis of steel structures with Eurocode 3 material model", *Journal of Structural Fire Engineering*, 2016; 7(3), 234-248.

[26] EN 1999-1-2:2007, *"Eurocode 9: Design of aluminium structures - Part 1-2: Structural fire design"*, European Committee for Standardization, Brussels, 2007.

Figure Captions

Figure 1: Layout of the rheological model: (a) Constitutive components (b) General stress-strain relationships for both springs at a prescribed temperature level.

Figure 2: Comparison between test results [12] and predictions of the rheological model for stress-related strain.

Figure 3: Comparison: (a) Strain output for different values of parameter ε_{u2} at 400°C, K=1300000 (b) Strain output for different values of parameter K at 400°C, ε_{u2}=0.49%

Figure 4: Performance of the rheological model at 400°C and comparison with results from [12].

Figure 5: Performance of the rheological model at 500°C and comparison with results from [12].

Figure 6: Performance of the rheological model at 600°C and comparison with results from [12].

Figure 7: Models for Springs 1 and 2 at: (a) 400°C , (b) 500°C , (c) 600°C.

Figure 8: Comparison between the test results [16] and predictions of the rheological model for stress-related strain.

Figure 9: Performance of the rheological model for aluminium at 200°C.

Figure 10: Performance of the rheological model for aluminium at 250°C.

Figure 11: Performance of the rheological model for aluminium at 300°C for stress level of $0.30\sigma_{1max}$: (a) K=77000.0 , (b) $\sigma_{2max} = 0.16\sigma_{1max}$.

Figure 12: Performance of the rheological model at 300°C for stress level of $0.50\sigma_{1max}$: (a) K=16000.0 , (b) $\sigma_{2max} = 0.16\sigma_{1max}$.

Figure 13: Model for Springs 1 and 2 at: (a) 200°C, (b) 250°C, (c) 300°C.

Figure 14: Performance of the rheological model for grade S275JR for 400°C: stress levels of $0.90\sigma_{1max}$, $0.80\sigma_{1max}$ and $0.70\sigma_{1max}$.

Figure 15: Performance of the rheological model for grade EN6082AW T6 for 200°C - stress levels of $0.28\sigma_{1max}$ and $0.42\sigma_{1max}$.

Table Captions

Table 1: Mechanical properties of S275JR in the temperature range 400-600°C [12].

Table 2: Test results of stationary creep tests for S275JR [12].

Table 3: Values of the constant K for the proposed rheological model in case of steel S275JR.

Table 4: Mechanical properties of EN6082AW [16] in the temperature range 200-300°C.

Table 5: Test results of stationary creep tests of EN6082AW T6 [16].

Table 6: Values of the parameter K for alloy EN6082AW T6.

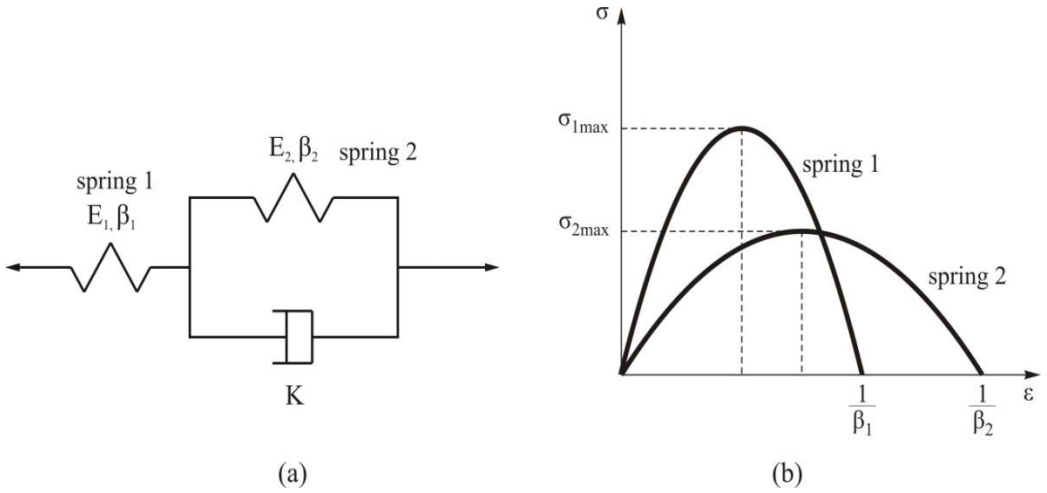
spring 1
E_1, β_1
E_2, β_2 spring 2
K
(a)
σ
σ_{1max}
σ_{2max}
spring 1
spring 2
$\frac{1}{\beta_1}$
$\frac{1}{\beta_2}$
ε
(b)

Figure 1

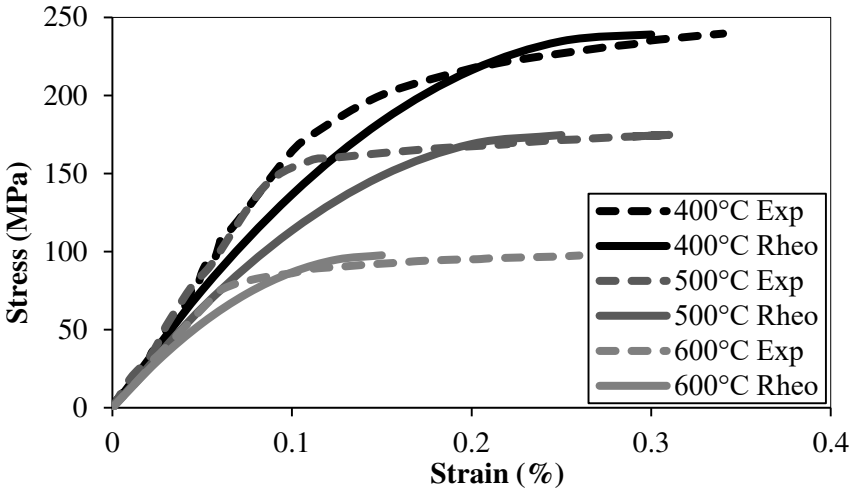
250
200
150
100
50
0
Stress (MPa)
0
0.1
0.2
0.3
0.4
Strain (%)
400°C Exp
400°C Rheo
500°C Exp
500°C Rheo
600°C Exp
600°C Rheo

Figure 2

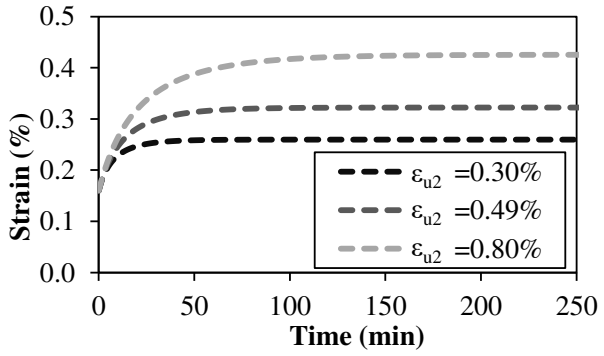
0.5
0.4
0.3
0.2
0.1
0.0
Strain (%)
0
50
100
150
200
250
Time (min)
εu2 =0.30%
εu2 =0.49%
εu2 =0.80%

(a)

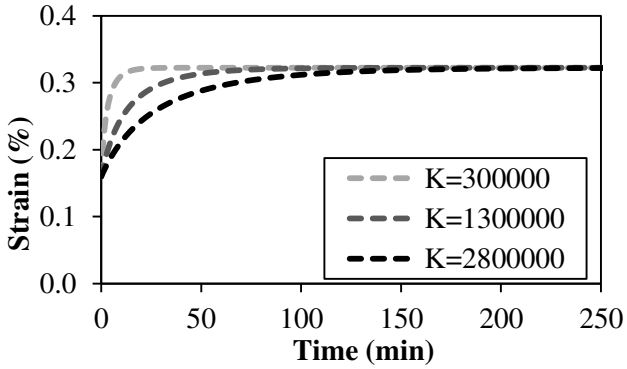
0.4
0.3
0.2
0.1
0.0
Strain (%)
0
50
100
150
200
250
Time (min)
K=300000
K=1300000
K=2800000

(b)

Figure 3

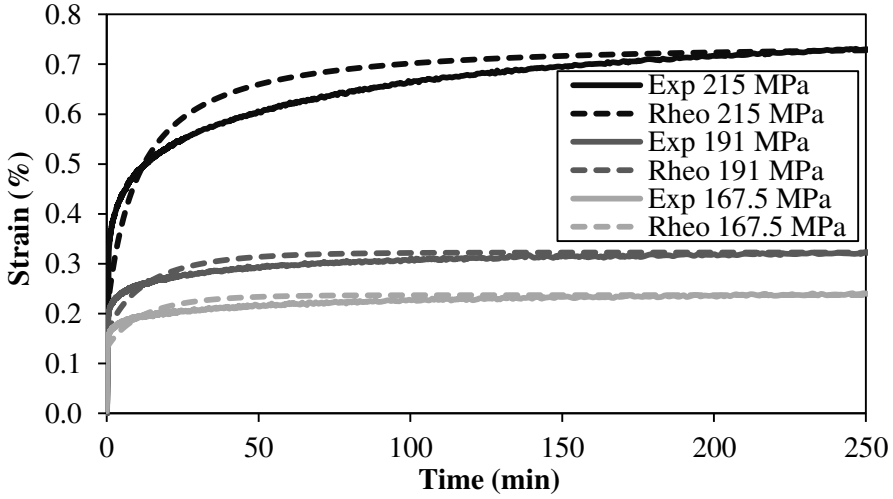
0.8
0.7
0.6
0.5
0.4
0.3
0.2
0.1
0.0
Strain (%)
0
50
100
150
200
250
Time (min)
Exp 215 MPa
Rheo 215 MPa
Exp 191 MPa
Rheo 191 MPa
Exp 167.5 MPa
Rheo 167.5 MPa

Figure 4

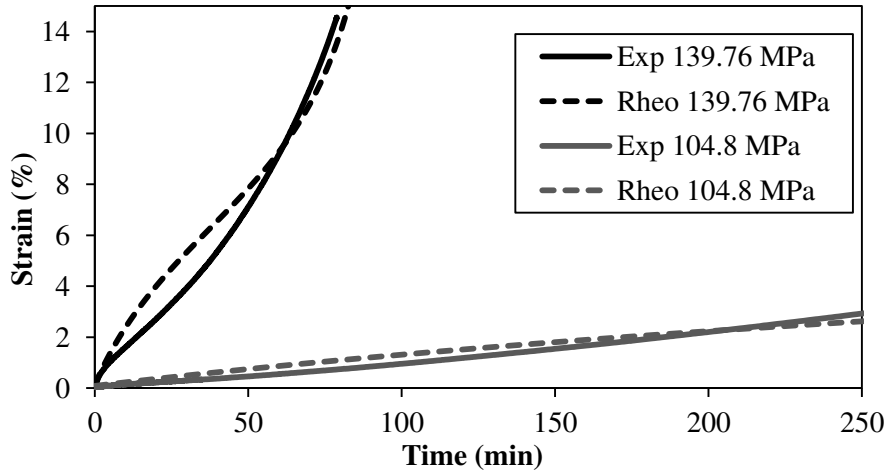
Exp 139.76 MPa
Rheo 139.76 MPa
Exp 104.8 MPa
Rheo 104.8 MPa
Strain (%)
Time (min)
0
2
4
6
8
10
12
14
0
50
100
150
200
250

(a)

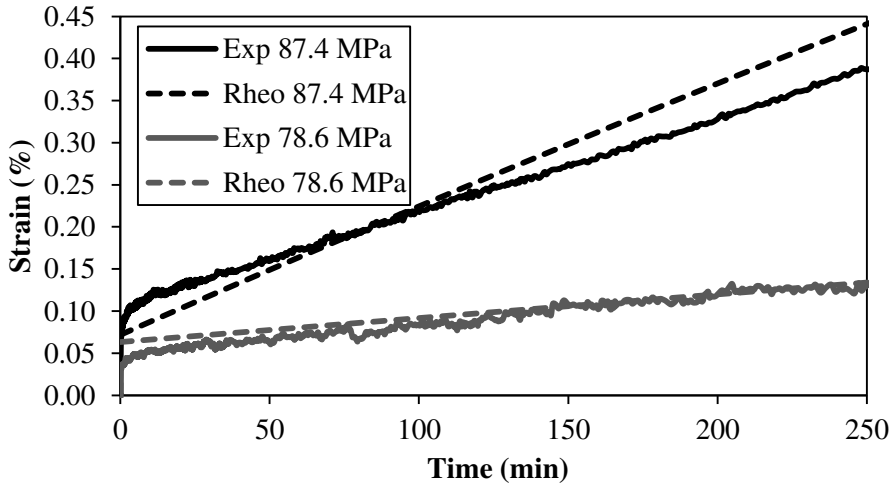
Exp 87.4 MPa
Rheo 87.4 MPa
Exp 78.6 MPa
Rheo 78.6 MPa
Strain (%)
Time (min)
0.00
0.05
0.10
0.15
0.20
0.25
0.30
0.35
0.40
0.45
0
50
100
150
200
250

(b)

Figure 5

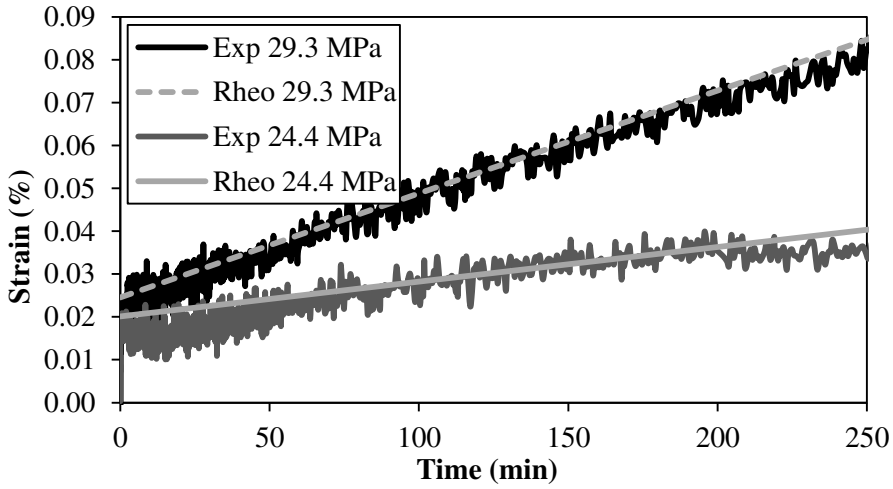
Exp 29.3 MPa
Rheo 29.3 MPa
Exp 24.4 MPa
Rheo 24.4 MPa
Strain (%)
Time (min)
0.00
0.01
0.02
0.03
0.04
0.05
0.06
0.07
0.08
0.09
0
50
100
150
200
250

(a)

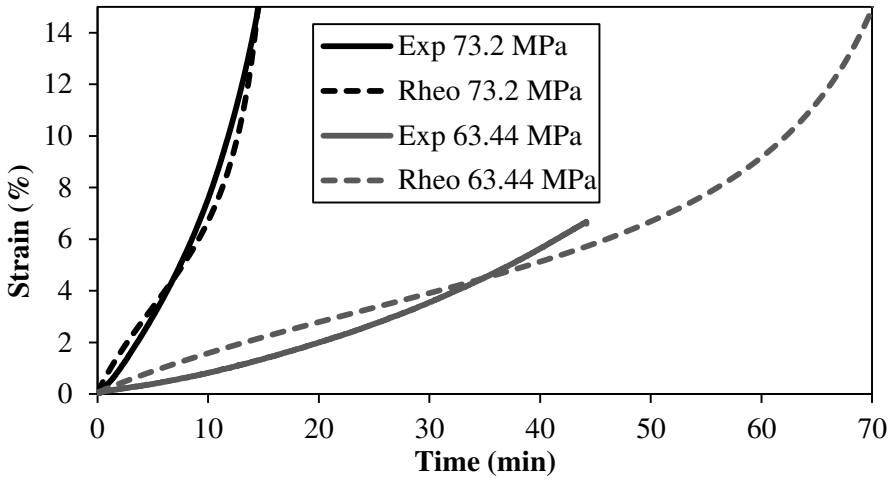
Exp 73.2 MPa
Rheo 73.2 MPa
Exp 63.44 MPa
Rheo 63.44 MPa
Strain (%)
Time (min)
0
2
4
6
8
10
12
14
0
10
20
30
40
50
60
70

(b)

Figure 6

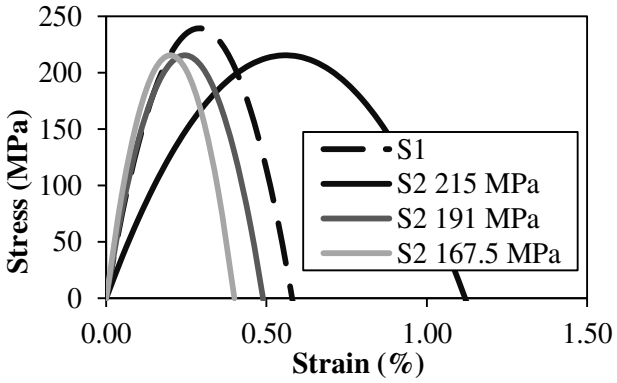
250
200
150
100
50
0
Stress (MPa)
0.00
0.50
1.00
1.50
Strain (%)
S1
S2 215 MPa
S2 191 MPa
S2 167.5 MPa

(a)

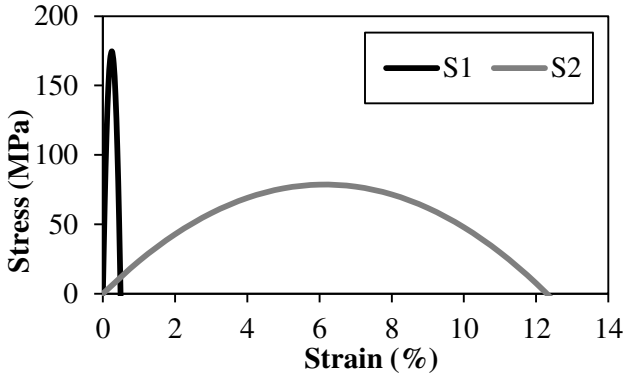
200
150
100
50
0
Stress (MPa)
0
2
4
6
8
10
12
14
Strain (%)
S1
S2

(b)

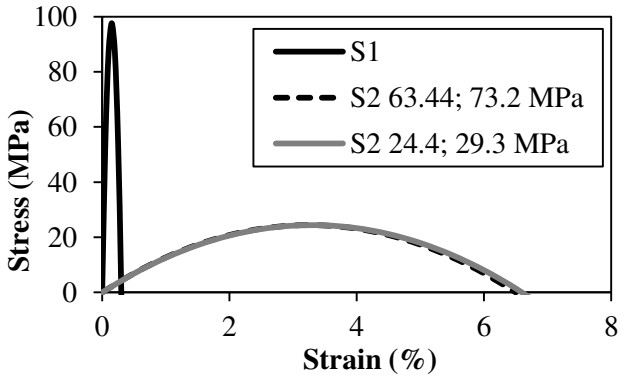
100
80
60
40
20
0
Stress (MPa)
0
2
4
6
8
Strain (%)
S1
S2 63.44; 73.2 MPa
S2 24.4; 29.3 MPa

(c)

Figure 7

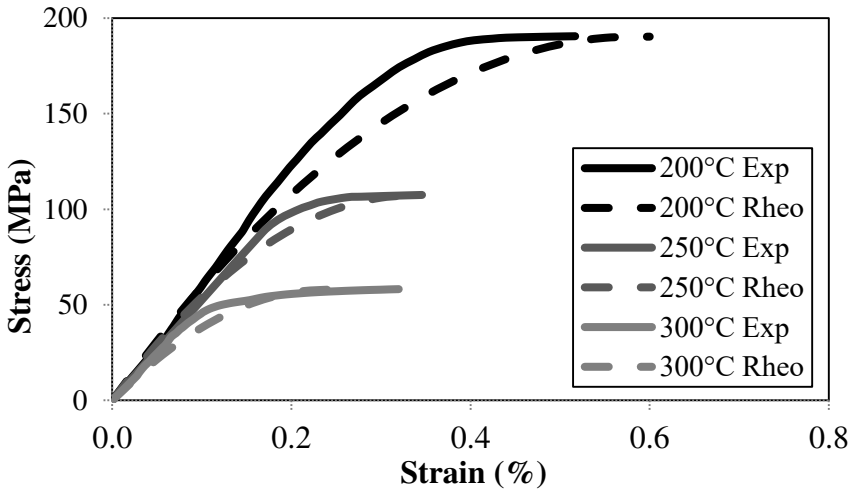
200
150
100
50
0
Stress (MPa)
0.0
0.2
0.4
0.6
0.8
Strain (%)
200°C Exp
200°C Rheo
250°C Exp
250°C Rheo
300°C Exp
300°C Rheo

Figure 8

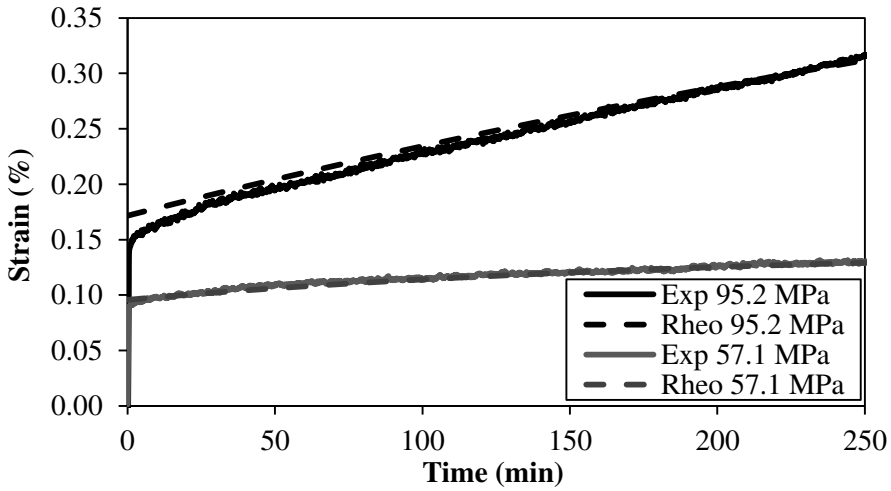
0.35
0.30
0.25
0.20
0.15
0.10
0.05
0.00
Strain (%)
0
50
100
150
200
250
Time (min)
Exp 95.2 MPa
Rheo 95.2 MPa
Exp 57.1 MPa
Rheo 57.1 MPa

Figure 9

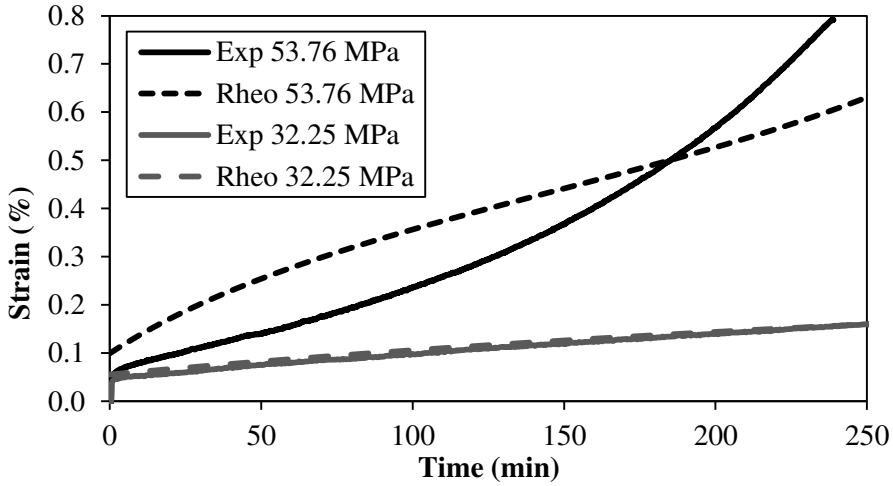
Exp 53.76 MPa
Rheo 53.76 MPa
Exp 32.25 MPa
Rheo 32.25 MPa
Strain (%)
Time (min)
0.0
0.1
0.2
0.3
0.4
0.5
0.6
0.7
0.8
0
50
100
150
200
250

Figure 10

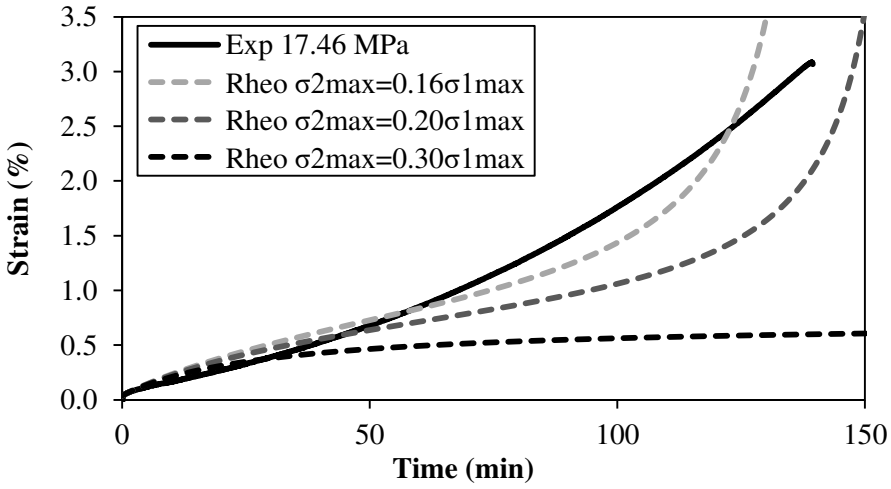
Exp 17.46 MPa
Rheo σ2max=0.16σ1max
Rheo σ2max=0.20σ1max
Rheo σ2max=0.30σ1max
Strain (%)
Time (min)
0.0
0.5
1.0
1.5
2.0
2.5
3.0
3.5
0
50
100
150

(a)

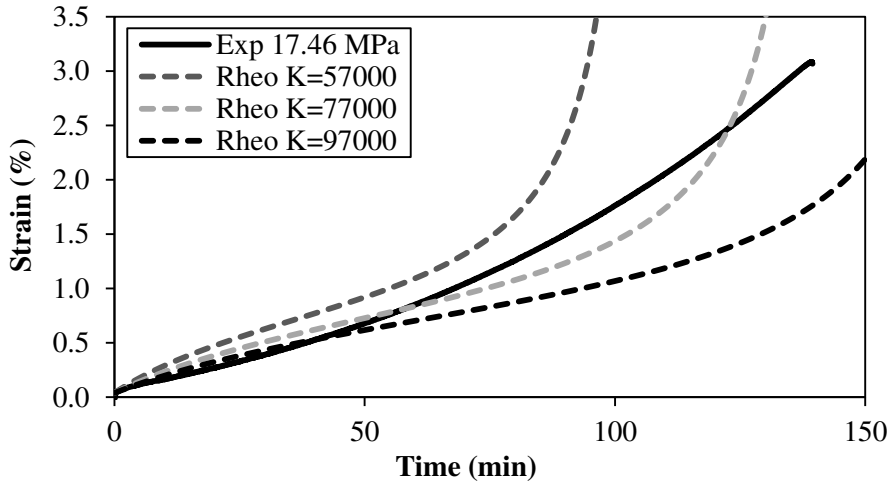
Exp 17.46 MPa
Rheo K=57000
Rheo K=77000
Rheo K=97000
Strain (%)
Time (min)
0.0
0.5
1.0
1.5
2.0
2.5
3.0
3.5
0
50
100
150

(b)

Figure 11

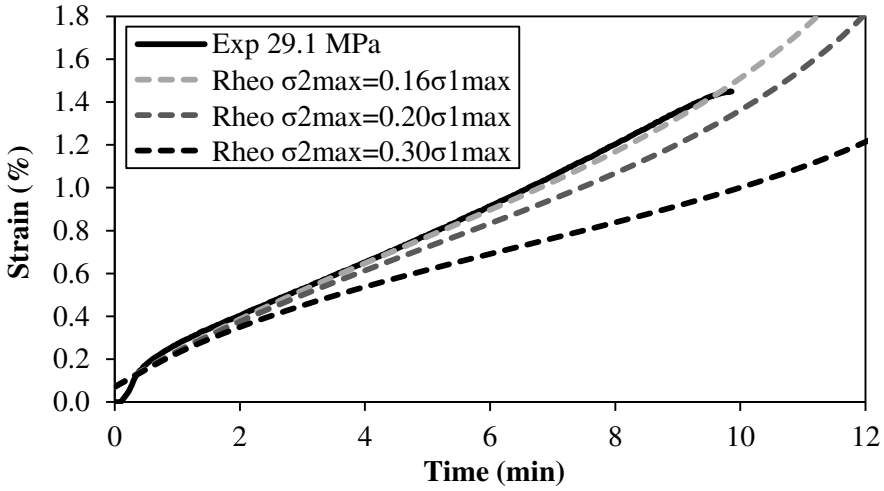
Exp 29.1 MPa
Rheo σ2max=0.16σ1max
Rheo σ2max=0.20σ1max
Rheo σ2max=0.30σ1max
Strain (%)
Time (min)
0.0
0.2
0.4
0.6
0.8
1.0
1.2
1.4
1.6
1.8
0
2
4
6
8
10
12

(a)

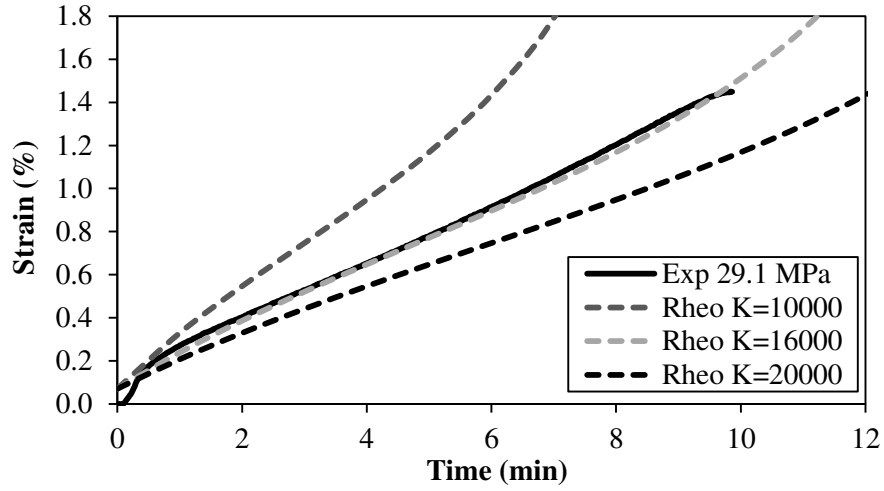
Exp 29.1 MPa
Rheo K=10000
Rheo K=16000
Rheo K=20000
Strain (%)
Time (min)
0.0
0.2
0.4
0.6
0.8
1.0
1.2
1.4
1.6
1.8
0
2
4
6
8
10
12

(b)

Figure 12

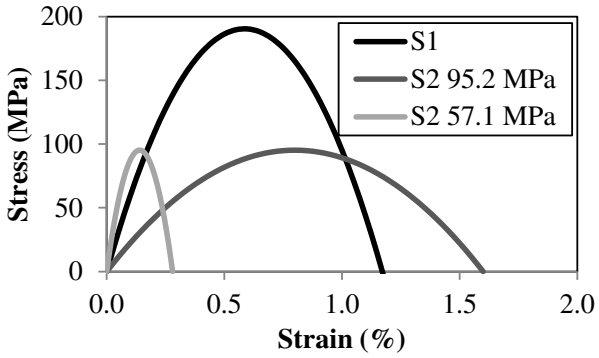

(a)

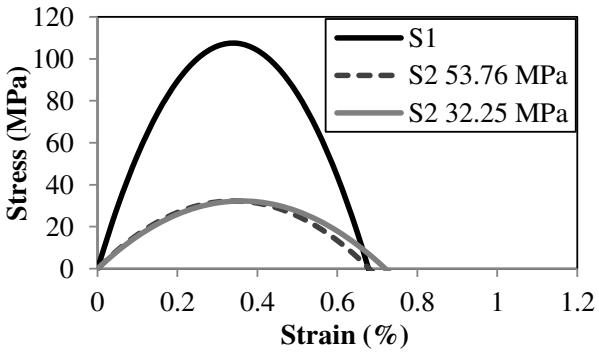

(b)

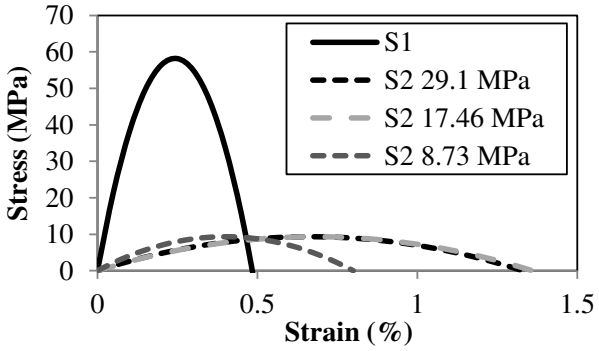

(c)

Figure 13

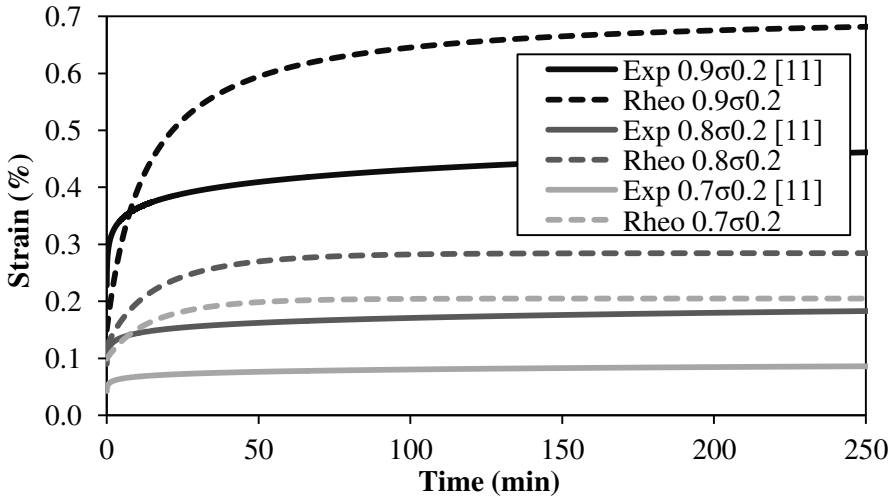
0.7
0.6
0.5
0.4
0.3
0.2
0.1
0.0
Strain (%)
0
50
100
150
200
250
Time (min)
Exp 0.9σ0.2 [11]
Rheo 0.9σ0.2
Exp 0.8σ0.2 [11]
Rheo 0.8σ0.2
Exp 0.7σ0.2 [11]
Rheo 0.7σ0.2

Figure 14

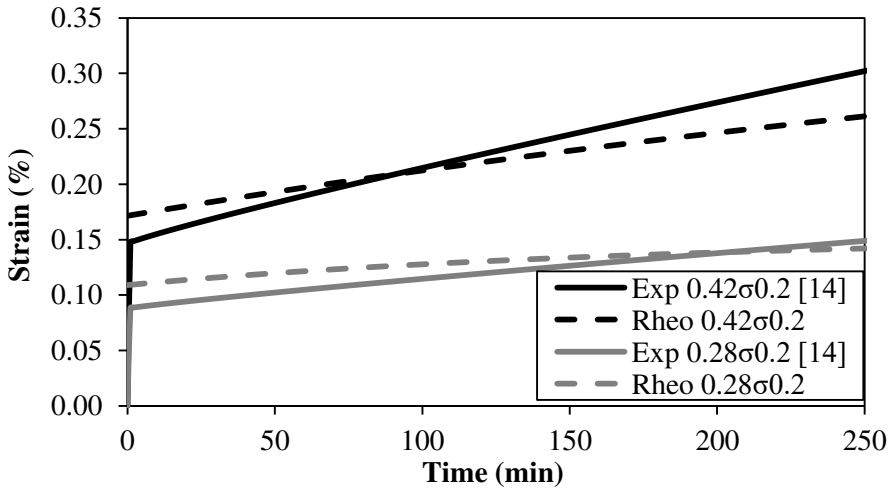
0.35
0.30
0.25
0.20
0.15
0.10
0.05
0.00
Strain (%)
0
50
100
150
200
250
Time (min)
Exp 0.42σ0.2 [14]
Rheo 0.42σ0.2
Exp 0.28σ0.2 [14]
Rheo 0.28σ0.2

Figure 15

Table 1

Temperature (°C)	**Modulus of elasticity E_1 (GPa)**	**Yield strength σ_{1max} (MPa)**
20	204.7	287.5
400	164.9	239.3
500	142.7	174.7
600	130.0	97.6

Table 2

Temperature	Stress σ_0 (MPa)	σ_0/σ_{1max}	Maximum strain ε_{max} (%)	Creep phase
400°C	167.5	0.7	-	Primary
	191.0	0.8	-	Primary
	215.0	0.9	-	Primary
500°C	78.6	0.45	0.7	Tertiary
	87.4	0.5	2.9	Tertiary
	104.8	0.6	12.4	Tertiary
	139.8	0.8	14.6	Tertiary
600°C	24.4	0.25	0.1	Tertiary
	29.3	0.30	0.5	Tertiary
	63.4	0.65	6.6	Tertiary
	73.2	0.75	22.5	Tertiary

Table 3

Temperature	σ_0/σ_{1max}	K
400°C	0.7	1700000.0
	0.8	1300000.0
	0.9	400000.0
500°C	0.45	27500000.0
	0.5	5600000.0
	0.6	730000.0
	0.8	50000.0
600°C	0.25	30000000.0
	0.30	12000000.0
	0.65	35000.0
	0.75	8500.0

Table 4

Temperature (°C)	**Modulus of elasticity E_1 (GPa)**	**Yield strength σ_{1max} (MPa)**
20	71.0	288.0
200	65.0	190.4
250	63.4	107.5
300	48.0	58.2

Table 5

Temperature	Stress σ_0 (MPa)	σ_0/σ_{1max}	Maximum strain ε_{max} (%)	Creep phase
200°C	38.10	0.20	-	No creep
	57.10	0.30	-	Primary
	95.20	0.50	1.80	Tertiary
250°C	16.13	0.15	-	No creep
	32.25	0.30	1.07	Tertiary
	53.76	0.50	0.78	Tertiary
300°C	8.73	0.15	-	Primary
	17.46	0.30	3.07	Tertiary
	29.10	0.50	1.45	Tertiary

Table 6

Temperature	σ_0/σ_{1max}	K
200°C	0.30	24000000.0
	0.50	14000000.0
250°C	0.30	5500000.0
	0.50	1300000.0
300°C	0.15	1900000.0
	0.30	77000.0
	0.50	16000.0